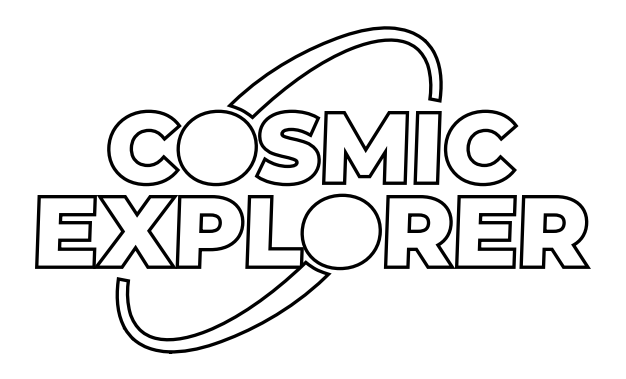
Technical Note CE-T2400012-01 2024/07/24

Cosmic Explorer corner layouts:
design considerations and down
selection

CE Optical Design Team

This is an internal working note of the COSMIC EXPLORER project.



http://www.cosmicexplorer.org/

CE-T2400012-01

Contents

1	The	The scope of alternative layout considerations				
2	Cor	re optic naming conventions	3			
3	Overview of layouts considered					
	3.1	Layouts with 45° angle of incidence on the beamsplitter	4			
		3.1.1 aLIGO	4			
		3.1.2 Split Telescope	4			
		3.1.3 Long Split Telescope	4			
		3.1.4 Reverse aLIGO	6			
		3.1.5 Long Reverse aLIGO	6			
		3.1.6 ITM Lens	6			
	3.2	Layouts with small angle of incidence on the beamsplitter	6			
		3.2.1 Shoelaces 1	7			
		3.2.2 Long Shoelaces 1	7			
		3.2.3 Shoelaces 2	7			
		3.2.4 Shoelaces 3	7			
		3.2.5 Crab 1	7			
		3.2.6 Long Crab 1	7			
		3.2.7 Crab 2	7			
4	Evaluation of corner layouts					
	4.1	Signal Extraction Cavity length	8			
	4.2	SEC loss	9			
	4.3	Beam splitter thermal distortions	10			
	4.4	Beamsplitter beam size	10			
	4.5	Beamsplitter Rayleigh range	11			
	4.6	Mode sensing and control actuation points	12			
	4.7	Stray light performance	13			
	4.8	Infrastructure impacts	14			
5	Ado	ditional considerations for optical layouts	15			
	5.1	Higher-order spatial mode coupling	15			
	5.2	Aberrations	15			
	5.3	ITM lens	15			
	5.4	Toroidal mirrors	16			
	5.5	Beamsplitter orientation	16			
	5.6	Arm cavity beam crossing point	17			
6	Pre	Preferred layouts and design concepts 1				
-	6.1	Long Crab 1	18			
	6.2	Long Reverse aLIGO	19			
A	Opt	tical design boundary conditions and assumptions	20			

1 The scope of alternative layout considerations

At the earliest stages of the CE conceptual design, we find it useful to take into consideration a broad range of possible interferometer layouts. First we introduce the scope of this document, and define some key terms. The term "layout" in this context refers to the number and ordering of core optics between the interferometer input (the power recycling mirror, or PRM) and the interferometer output (the signal extraction mirror or SEM), as well as their rough geometrical orientation with respect to each other, and whether they are flat of curved. We do not include any detailed geometric design of the recycling and extraction cavities themselves in this document, although certain boundary conditions on such designs imposed by different layouts are necessarily considered when evaluating layouts. All of the considered layouts constitute dual-recycled Fabry-Perot Michelson interferometers, with 90° angular separation between the arm cavities, and assume 40 km arm length where relevant.

In this document we introduce a number of alternative interferometer layouts, and explain how they can be categorized in terms of their key features. We describe some of the main considerations in evaluating the benefits and drawbacks of the different layouts, both from the point of view of interferometric performance, and compatibility with other subsystems such as vacuum infrastructure design. Finally, we make a recommendation for two preferred layouts to pursue at the next level of detailed optical design in the next phase of the conceptual optical design of the CE interferometers.

2 Core optic naming conventions

In discussing the different optical layouts that will be considered for CE, it is helpful to establish a convention for the naming of core optics components. Where possible, the same names are used as in aLIGO. In this spirit, the four arm cavity mirrors are ITMX, ETMX, ITMY and ETMY, the beamsplitter is BS, the power recycling mirror is PRM. All layouts contain the 6 aforementioned optics, along with a signal extraction mirror, SEM. In light of the way in which this mirror has always been used in aLIGO, and will be used in CE, we switch naming from the signal recycling mirror (SRM) to signal extraction mirror (SEM).

All additional core optics names adhere to the following naming conventions:

- If located between the power recycling mirror and the beamsplitter, optic names begin with PR (for Power Recycling).
- If located between the signal extraction mirror and the beamsplitter, optic names begin with SE (for Signal Extraction).
- If located between the beamsplitter and ITMX, optic names begin with MX (for Michelson X).
- If located between the beamsplitter and ITMY, optic names begin with MY (for Michelson Y).

- For PR mirrors other than PRM, the optic numbers increase from PRM towards the beamsplitter.
- For SE mirrors other than SEM, the optic numbers increase from SEM towards the beamsplitter.
- For MX and MY mirrors, the optic numbers increase from the beamsplitter towards the ITMs.

3 Overview of layouts considered

Figure 1 shows most of the layouts that were considered as part of this study. We do not include a detailed discussion of the pros and cons of each layout here, but instead save that discussion for Section 4.

3.1 Layouts with 45° angle of incidence on the beamsplitter

We begin with layouts which have the common feature of a 45° angle of incidence (AOI) at the BS. This is the AOI at the BS that has been used for all major gravitational wave detectors to date.

3.1.1 aLIGO

The **aLIGO** layout is the same as the core layout of Advanced LIGO. In the corner region of the interferometer, the only optics which are specific to the X and Y arms are the ITMs themselves. The beam size at the BS is roughly equivalent to the beam size at the ITMs, unless the ITMs are equipped with curved antireflective (AR) surfaces, which provide some lensing and beam compression between the ITM and the BS, depending on the physical separation of these optics. With the beamsplitter being probed under 45° angle of incidence, the effective beam size in the tangential plane is $\sqrt{2}$ times bigger than in the sagittal plane. The beam reducing telescopes are located between the PRM and the BS, and between the BS and the SEM.

3.1.2 Split Telescope

The **Split Telescope** layout is something of a compromise between the aLIGO layout and the Reverse aLIGO layout. The BS is located effectively inside the beam reducing telescopes. As such, there is one optic specific to each of the X and Y arms in addition to the ITMs themselves, and one optic specific to the PRC and SEC other than the PRM and SEM themselves. In this layout, the beam size on the BS can be made smaller than in the aLIGO layout.

3.1.3 Long Split Telescope

The **Long Split Telescope** layout is a modified version of Split Telescope, with two additional optics in the PRC. This feature allows independent mode matching capability for the PRC and SEC to the common arm mode of the interferometer.

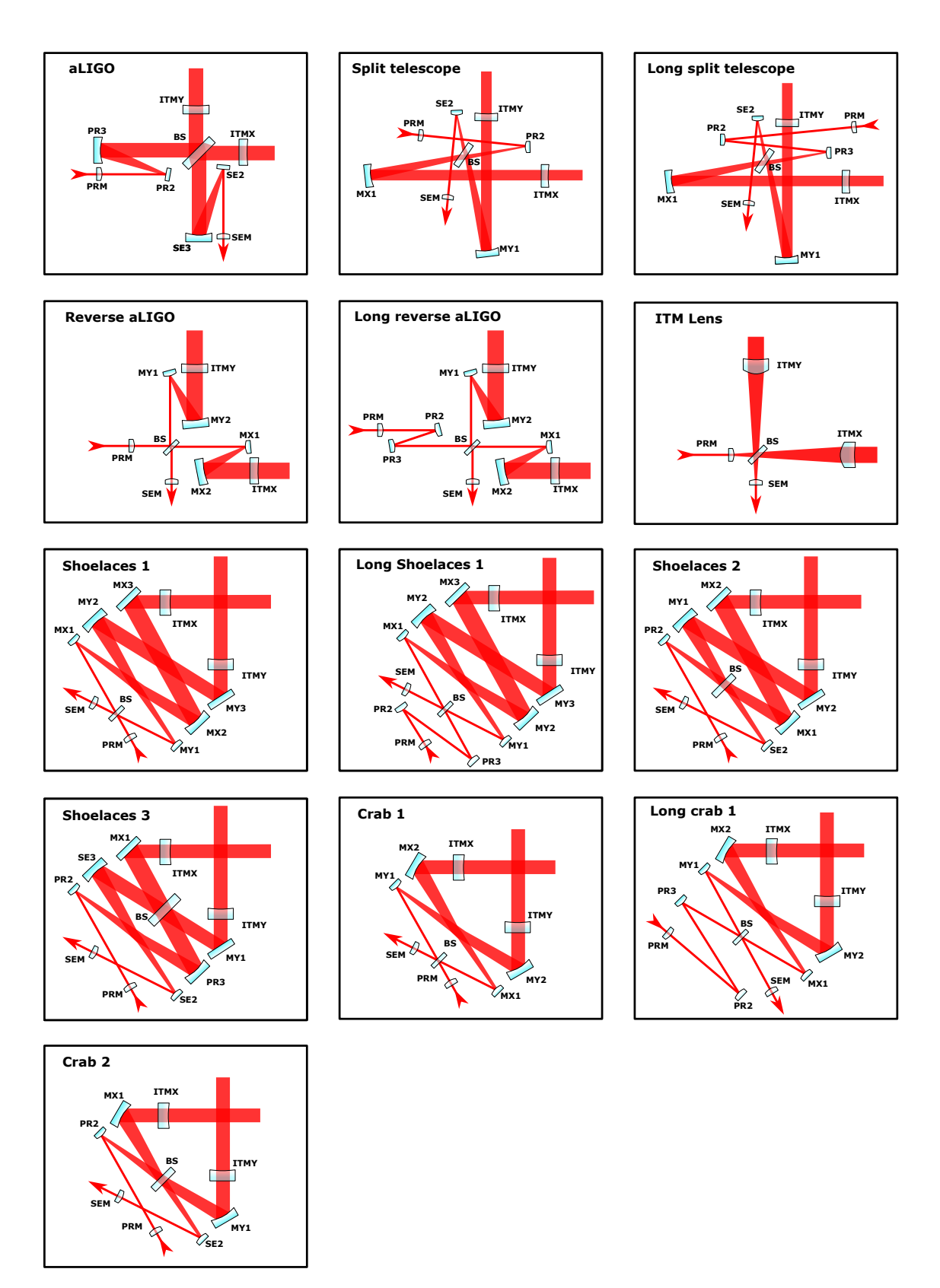


Figure 1: Illustration of the many optical layouts considered for the CE interferometers. The sketches are not to scale, and may not reflect the actual geometry of a more detailed design conforming to the layout.

3.1.4 Reverse aLIGO

The Reverse aLIGO layout is the one originally presented in the CE Horizon Study. In this layout, the beam reducing telescopes are located between the BS and the ITMs. In this way, this layout has two optics which are specific to each of the X and Y arms in addition to the ITMs themselves. On the other hand, PRM and SEM themselves are the only optics specific to the PRC and SEC respectively. In this layout, the beam size on the BS can be made much smaller than in the aLIGO layout.

3.1.5 Long Reverse aLIGO

The Long Reverse aLIGO layout is a modified version of Reverse aLIGO, with two additional optics in the PRC. This feature allows independent mode matching capability for the PRC and SEC to the common arm mode of the interferometer.

3.1.6 ITM Lens

The ITM Lens layout uses a minimal number of optics. A lens figured into the ITM AR surface is used to converge the beams from the X and Y arms through the BS towards the PRM and SEM. Other than the ITMs themselves, there are no arm-specific optics in the corner region of the interferometer. Other than the PRM and SEM themselves, there are no recycling/extraction cavity-specific optics in this layout.

3.2 Layouts with small angle of incidence on the beamsplitter

We continue with layouts which have the common feature of a low (\sim 1°) AOI at the BS. As discussed further in Sec. 4 and in [1], this feature may provide some benefits in terms of thermal lensing in the BS and associated mode mismatch.

The first broad class of such layouts are named 'Shoelaces' after the appearance of the multiple crossing beam paths. In each of these layouts flat folding mirrors are used to direct the beams from the X and Y arms towards the next optics in the corner interferometer (either the BS or additional curved folding mirrors). The AOI on the flat folding mirrors is necessarily close to 22.5° , so as to maintain a low AOI on the next folding mirror and/or the BS. The $\sim 22.5^{\circ}$ AOI on the flat folding mirrors leads to a slightly larger effective beam size on these mirrors, at $\cos^{-1}(22.5^{\circ})=1.08$ times the ITM beam size.

The second class of low-AOI layouts are named 'Crab', for fairly obvious reasons. In each of these layouts the folding mirrors used to direct the beams from the X and Y arms towards the next optics in the corner interferometer (either the BS or additional curved folding mirrors) are not assumed to be flat, but may be curved to provide some beam focusing. Since the AOI on these optics must be close to 22.5° (for the same reasons as the Shoelaces layouts) it is clear that significant astigmatism can be introduced: the effective RoC in tangential and sagittal planes differ by $\sim 100 \times (1 - \cos^2{(22.5^{\circ})}) = 14\%$. These layouts therefore require the use of toroidal mirrors with different actual RoCs in tangential and sagittal planes for astigmatism compensation, or offloading of the focusing power of these folding mirrors to a strong lens in the ITM.

3.2.1 Shoelaces 1

The **Shoelaces 1** layout is close to a low-AOI version of the Reverse aLIGO layout. This layout can provide a small beam size and a low AOI at the BS, as well as providing 3 arm cavity-specific core optics for each arm in addition to the ITMs themselves. It contains only the PRM and SEM themselves as recycling/extraction cavity-specific optics, however.

3.2.2 Long Shoelaces 1

The **Long Shoelaces 1** layout is close to a low-AOI version of the Long Reverse aLIGO layout. The additional optics in the PRC allow for independent actuation of the mode in the PRC from that of the SEC.

3.2.3 Shoelaces 2

The Shoelaces 2 layout is close to a low-AOI version of the Split Telescope aLIGO layout. The BS is located inside the beam reducing telescopes, and as such the beam size at the BS can be made considerably smaller than at the ITMs. This layout provides two arm cavity-specific core optics per arm in addition to the ITMs, as well as one recycling/extraction cavity optic in addition to the PRM/SEM.

3.2.4 Shoelaces 3

The Shoelaces 3 layout is the closest low-AOI layout to the aLIGO layout in terms of topology. The flat folding mirrors MX1 and MY1 are used to direct the beams from the X and Y arms toward the BS at a low AOI. With a low AOI on the BS, the effective beam size on the BS is roughly equivalent between tangential and sagittal planes. Furthermore, unless a strong ITM lens is assumed, the beam size on the BS will be roughly equal to the beam size on the ITMs. The MX1 and MX2 optics are each specific to the X and Y arms respectively. As in the aLIGO layout, the Shoelaces 3 layout also boasts two recycling/extraction cavity-specific optics in addition to the PRM and SEM.

3.2.5 Crab 1

The Crab 1 layout is effectively a low-AOI version of the Reverse aLIGO layout.

3.2.6 Long Crab 1

The Long Crab 1 layout is effectively a low-AOI version of the Long Reverse aLIGO layout.

3.2.7 Crab 2

The Crab 2 layout is effectively a low-AOI version of the Split Telescope layout.

4 Evaluation of corner layouts

It was not deemed an efficient use of resources to make detailed optical designs for all of the corner layouts described in Sec. 3. Instead, we highlighted some of the major considerations

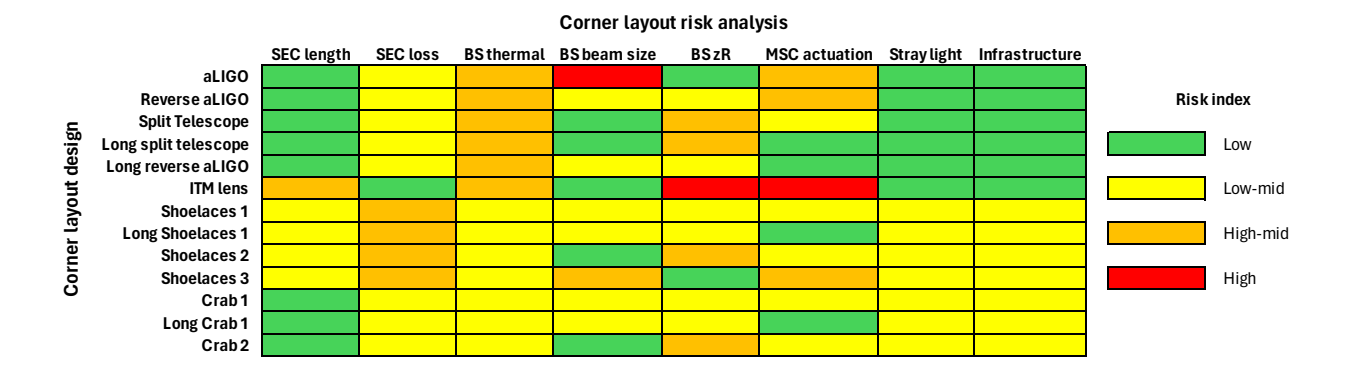


Figure 2: Risk chart for different corner layouts in terms of the major considerations outlined in this document. Risk level increases from green (lowest risk) through yellow and orange to red (highest risk).

that would go into an evaluation of the prospects of each layout. These criteria were then used for a down selection to a smaller number of layouts, which could then be pursued with more detailed designs. Figure 2 shows an evaluation of each of the corner layout designs referenced in Sec. 3 in terms of these major design considerations. The assessed risk of each layout in terms of each consideration is color coded from lowest risk (green) to highest risk (red). However, we do not attempt to convey the relative importance of different considerations in Fig. 2. The true evaluation of different layouts is naturally more subtle than a simple summation of risk factors. In some cases, there are additional layout-specific design constraints that are not captured by the overall considerations addressed in this section. Nonetheless, the table does give a useful guide, and is a helpful "at a glance" reference to compare different layouts. The remainder of this section addresses each consideration in turn, and discusses the reasoning behind the risk assessment categories assigned to each layout. Additional layout-specific considerations will be discussed in Section 5.

4.1 Signal Extraction Cavity length

All other things being equal, the SEC resonance frequency will be lower in CE than in aLIGO by roughly a factor of 10, due to the 10 times longer arms. This brings the resonance into the detection band, where in the RSE configuration it reduces sensitivity to gravitational waves from the postmerger phase of binary systems [2]. Specifically, the SEC resonance frequency is approximately

$$\frac{c}{2} \frac{1}{\sqrt{2\pi \mathcal{F}_a L_a L_s}},\tag{1}$$

where \mathcal{F}_a is the arm cavity finesse, and L_a, L_s are the arm cavity length and SEC length respectively. To keep this resonance frequency high enough, the SEC length must be kept shorter than about 200 m for the 40 km CE interferometer (90 m for the 20 km CE interferometer). This constrains the corner layout designs, generally placing a penalty on any beam path between ITMs and BS over which the beam parameter is not evolving significantly. It should also be noted that while 200 m is assumed as an upper limit for the SEC length in the 40 km interferometer, shorter is generally preferred, although the performance degrada-

tion for longer lengths is somewhat graceful by virtue of the $1/\sqrt{L_s}$ dependence of the SEC resonance frequency.

Without getting into the detailed design of the SEC for each layout, it is possible to say that in principle almost all layouts could be made to fit within the 200 m upper limit for SEC length. As such, we have not found this consideration to be particularly high priority in distinguishing between most layouts. Nonetheless, we can identify some advantages and disadvantages in this respect between the different layouts.

We can also show that specifically the ITM Lens layout is mutually incompatible with the SEC length and BS Rayleigh range conditions. This will be discussed further later in this section, once the BS Rayleigh range design consideration has been properly introduced. For now, it will suffice to say that this puts the ITM Lens layout in the high-risk category for SEC length.

Less severe risk in terms of SEC length are associated with the Shoelaces 1, 2 and 3 layouts by virtue of their inclusion of additional un-powered folding mirrors between the ITMs and BS (MX/Y3, MX/Y2 and MX/Y1, respectively for Shoelaces 1, 2 and 3). This additional folding mirror will likely add several 10s of meters of length to the SEC, because the beam does not begin converging until it reflects off the next mirror towards the BS (MX/Y2, MX/Y1 and PR/SE3 respectively for Shoelaces 1, 2 and 3). This risk could be mitigated however by allowing for an ITM substrate lens, which would begin the beam convergence immediately upon exiting the arm cavities.

The remaining layouts are assigned a low risk with regards to the SEC length constraint.

4.2 SEC loss

The CE interferometer noise budget assumes 1.5 MW of circulating arm power, and 10 dB of effective squeezing. To achieve this level of effective squeezing requires SEC losses to be kept below around 500 ppm per round trip [3]. This loss budget includes scatter and absorptive losses within the SEC, as well as transmission through SEC mirrors and reflection off BS and ITM AR surfaces. It does not, however, include losses due to mode mismatch or other low-order wavefront errors, which impact the interferometer performance in different, potentially more severe, ways.

At this stage of the conceptual design process, we have not performed a detailed optical loss analysis for each of the proposed layouts. Some common considerations to reduce optical loss in all layouts include the assumption that we will not include compensation plates for the ITMs, and that wherever possible low optical absorption materials will be used inside the SEC. Optical surfaces will be polished to appropriate specifications to achieve the scattering loss goals, and optic sizes will be compatible with low clipping losses within a range of alignment scenarios. Nonetheless some distinction can be made between optical layouts based simply on the number of optics present in the SEC, each of which will necessarily contribute some optical loss.

We therefore assign risk ratings for the different layouts based on this number. The SEC in the ITM Lens layout has just the SEM itself, along with the ITMs and the BS, and therefore receives the lowest risk rating in this category. All other layouts except Shoelaces

types include an additional two optics in the SEC, and therefore receive the next lowest risk rating. The Shoelaces layouts include three optics in the SEC in addition to the SEM and ITMs, so these are assigned a slightly higher risk rating. In the end there may be layout-independent factors that have a stronger bearing on the SEC loss, so we do not see the SEC loss as a strongly distinguishing consideration between different layouts at this stage.

4.3 Beam splitter thermal distortions

With a target arm circulating power of 1.5 MW, and a nominal arm cavity finesse of 450, we expect optical power of around 5.2 kW incident on the beamsplitter from each of the two short Michelson arms. This corresponds to 10.4 kW incident on the BS from the PRC side.

Thermal distortions at the BS can have a significant impact on the contrast defect, and on higher-order mode couplings within the interferometer [1]. Simulation studies have shown that it will be necessary to perform some thermal correction at the BS in order to meet the 500 ppm SEC loss target[†]. Assuming that correction is needed, the same studies have shown the correction to be more effective in the case of low AOI at the BS. This is understood to be because the beams passing through the BS substrate (from the PRC to the one arm cavity and from the SEC to the other arm cavity) follow a more common path in the case of low AOI than in the 45° AOI case.

Although the thermal distortions are larger in magnitude for a smaller beam size, thermal distortions also have a smaller relative impact on the spatial modal content of smaller beams. To first order at least, these factors cancel out, such that the beam size at the beamsplitter has no impact on the effect of thermal distortions on the interferometer performance. More detailed modeling should be pursued to confirm this in the case of residual distortions after correction, but at this stage we do not consider the beam size at the BS to be a distinguishing factor between layouts in terms of the BS thermal distortion consideration.

Based on the results of this modeling we therefore assign all low AOI layouts a moderate risk rating, and all 45° layouts a slightly higher risk rating. There are no layouts with low risk with regards to this consideration, indicating that this is a high priority topic for further study.

4.4 Beamsplitter beam size

The CE 40 km interferometer ITMs already go beyond the limits of what is available in terms of aperture and mass for the highest grade fused silica that can be produced by Heraeus [?]. When the BS is probed under a 45° AOI, the effective beam size in the tangential plane is $\sqrt{2}$ times bigger than the actual beam size. In the case of the aLIGO layout, this would lead to a required BS aperture of around 1 m, which is considered to be technically very challenging to produce. This places an upper bound on the effective beam size (related to the true beam size by $w_{\rm ITMeff} = w_{\rm ITM}/\cos(\theta_{i\rm BS})$.) of 12 cm. A lower bound on the effective

[†]For the purpose of this discussion, the higher-order mode coupling caused by BS thermal distortions is not included in the SEC loss budget, since it is known to have a more insidious impact on the interferometer performance via squeezed light dephasing. However, casting the BS thermal distortion effects in terms of SEC loss is still helpful in establishing a relative risk between different optical layouts.

beam size at the BS arises when considering thermorefractive noise at the BS [4]. For the CE 40 km interferometer, we take this lower bound to be 1 cm.

The aLIGO layout is assessed as high risk due to the need for a 1 m scale BS substrate to handle the $\sim 17\,\mathrm{cm}$ effective beam size in the tangential plane. The Shoelaces 3 layout is assessed as high-mid risk due to the need for a 70 cm scale BS substrate. Naïvely this seems quite achievable based on the fact that we assume 70 cm scale ITMs to be achievable, but there are additional considerations which have not been fully explored, such as ghost beams and internal reflections within the BS. The low AOI mitigates some of these concerns again due to the small separation between the two beams present at the BS AR surface.

The low-mid risk layouts are all those in which the BS is placed after two powered optics have been encountered in the path from the arm cavities. In these cases the beam size reduction from the arms to the SEM has already been achieved by the interaction point with the BS, and in general a small beam waist is needed to gracefully accumulate Gouy phase to enable SEC geometrical stability. These layouts tend to push toward the lower bound of 1 cm beam size on the BS, which is why they are assigned low-mid risk.

The designs in which the BS is located in the region of initial convergence from the arms towards the SEM are lowest risk in terms of this consideration, because it is possible to choose almost any beam size between 12 cm and 1 cm by adjusting the position of the BS relative to the ITMs.

A secondary consideration for the BS beam size is the possible impact on the BS size itself on the mechanical mode frequencies. As shown in Ref. [5], for fixed substrate aspect ratio, the lowest frequency acoustic modes increase in frequency as the BS is made smaller. This is considered to be an additional advantage for small BS beam sizes, which would allow for a BS with smaller dimensions.

4.5 Beamsplitter Rayleigh range

Some layouts involve the beam parameter evolving rapidly in the vicinity of the BS (e.g. split telescope, Crab 2). In such a case, a BS placement offset produces a mode mismatch between the X and Y arms of the interferometer. This places tight tolerances on the precise placement of the BS as a result. The relationship between BS placement uncertainty/tolerance $\sigma_{z_{\rm BS}}$, tolerated loss due to mode mismatch L and the minimum beam Rayleigh range in the BS vicinity $z_{\rm R_{min}}$ is derived in Ref. [6] as

$$z_{\rm R_{\rm min}} = \frac{\sigma_{z_{\rm BS}}}{L}.$$
 (2)

Assuming a positioning uncertainty of 5 mm and a loss tolerance of 25 ppm, this constrains the Rayleigh range to be greater than 1 m. Missing factor 2?

For the ITM Lens layout, the focal length of the lens in the ITM sets the scale for the length of the SEC. The SEC must accumulate some Gouy phase in order to be stable, which means that the beam must be brought close to a waist. For a beam as large as the beam from the arm cavity, the waist produced by passing through a single ITM lens will effectively be at the focal point of the lens. With no other powered optics in the PRC or SEC, one can easily

derive the beam parameter of the PRC/SEC beam in terms of the ITM lens focal length f_{ITM} or focal power $s_{\text{ITM}} = 1/f_{\text{ITM}}$ and the initial beam parameter q_{ARM} as:

$$q_{\rm RC} = \frac{q_{\rm ARM}}{1 - q_{\rm ARM}/f_{\rm ITM}} = \frac{q_{\rm ARM}}{1 - s_{\rm ITM}q_{\rm ARM}}.$$
 (3)

Then solving for the focal power that produces a recycling cavity mode with Rayleigh range $z_{R_{\rm RC}}$:

$$s_{\text{ITM}}^{\text{max}} = \frac{L \pm \sqrt{L^2 + 4|q_{\text{ARM}}|^2 z_{R_{\text{ARM}}}/z_{R_{\text{RC}}}}}{2|q_{\text{ARM}}|^2},\tag{4}$$

where $\Im\{q_{\text{ARM}}\}=z_{R_{\text{ARM}}}$ and for a symmetric cavity $\Re\{q_{\text{ARM}}\}=L/2$, and therefore $|q_{\text{ARM}}|^2=L^2/4+z_{R_{\text{ARM}}}^2$, where $L=40\,\mathrm{km}$ is the arm length. We also assume for any reasonable optical design that $z_{R_{\text{ARM}}}\gg z_{R_{\text{RC}}}$.

For an initial beam parameter of $q_{\text{ARM}} = (20 + i\,14)\,\text{km}^{\dagger}$, and taking the minimum allowable $z_{R_{\text{RC}}} = 1\,\text{m}$, we recover a maximum positive focal power $s_{\text{ITM}}^{\text{min}} = 4.88\,\text{mD}$, corresponding to a minimum positive focal length solution $f_{\text{ITM}}^{\text{min}} = 205\,\text{m}$. Thus we see that in the case of the ITM lens design, the SEC length and BS Rayleigh range conditions can not be simultaneously met. This already effectively excludes the ITM Lens layout from further consideration, but at a minimum it places it in the high risk category for both SEC length and BS Rayleigh range considerations.

The next highest level of risk for this category is assigned to layouts in which the BS is placed is the primary region of beam reduction from the ITMs to the PRM/SEM, i.e. Split Telescope, Long Split Telescope, Shoelaces 2 and Crab 2. It is conceivable that the extra design flexibility afforded by the additional mirrors, when compared to ITM Lens, do allow these layouts to simultaneously meet both the BS beam size and BS z_R requirements. However, without going into the details of the SEC/PRC design, the challenge for these layouts is expected to be more in the direction of meeting the BS z_R requirement than the BS beam size requirement.

For the layouts in which the BS is placed next to the SEM, i.e. Reverse aLIGO, Long Reverse aLIGO, Crab 1, Long Crab 1, Shoelaces 1 and Long Shoelaces 1, the risk is assumed to be slightly less, at low-mid. For these layouts we assume that the majority of the beam reduction has already occurred closer to the ITMs, and that the Rayleigh range in the vicinity of the BS can therefore be made several meters, allowing for a graceful accumulation of Gouy phase between MX/Y1 and SEM.

Finally, the layouts with the largest beam size at the BS, i.e. aLIGO and Shoelaces 3, will have many kilometer long Rayleigh ranges in the BS vicinity, and thus present the lowest risk for this consideration.

4.6 Mode sensing and control actuation points

Experience from aLIGO operation has shown that it is important to have control over the eigenmodes of all of the core interferometer cavities in order to achieve maximal circulating

[†]See Appendix A.

light power in the arms [7]. This will be even more critical in CE, with greater circulating light power targets, and potentially greater susceptibility to mode mismatch due to the higher-order mode resonances lying in the detection band. This places a premium on layouts having sufficient actuation points within the PRC and SEC to independently mode match them to the arm cavities. We also require sufficient actuation points to match the arms to each other, minimizing contrast defect.

The ITM Lens layout is assigned a high risk in this category, because there are no mode sensing and control (MSC) actuation points available in the core interferometer outside of the ITMs, BS, PRM and SEM. While one could argue that there are also fewer possible sources of mode mismatch, in practice it has always been found that more actuators is preferable.

The aLIGO, Shoelaces 3, Reverse aLIGO, Crab 1 and Shoelaces 1 layouts have been assessed as high-mid risk in this category. For aLIGO and Shoelaces 3, this is because the ITMs are the only optics in the corner area that are specific to the X and Y arms. This means that all wavefront actuation to minimize contrast defect (and hence laser technical noise coupling) must occur at the ITMs themselves (or the ETMs). Especially in the absence of compensation plates, this is considered to be very challenging.

Reverse aLIGO, Crab 1 and Shoelaces 1 layouts are assessed as high-mid risk because the PRM and SEM are the only optics in the corner area that are specific to the PRC and SEC. Common-mode actuation of the other corner optics could be used to match the arm cavity mode to either the PRC or SEC, but in the case where PRC and SEC are not matched to each other, these layouts have insufficient actuation points to correct this. Ideally we would have two recycling/extraction cavity-specific optics that are separated by some Gouy phase to enable full mode control.

Split telescope, Shoelaces 2 and Crab 2 are assessed as mid-low risk in this category because they each have two or more arm-specific optics (MX/Y1 and ITMs) and two recycling/extraction cavity-specific optics (PRM, PR2, SEM and SE2). Naïvely this appears to allow full control of arm-to-arm matching, PRC to arm matching and SEC to arm matching. However, in realistic designs all arm-specific optics are located in positions with very little Gouv phase separation, making them degenerate actuators for a MSC system.

All of the 'long' layouts mitigate the risks associated with the high-mid risk layouts described above by adding two more PRC optics, which can be separated by some Gouy phase: PR2 and PR3. This should allow full MSC control for matching the PRC to the SEC, while maintaining two arm-specific optics with some reasonable Gouy phase separation to match the arms to each other and to the SEC. The penalty for adding optics PR2 and PR3 to the PRC is not high, because losses here are not as critical as in the SEC, and the PRC length is much less constrained than the SEC. The Long Reverse aLIGO, Long Crab 1, Long Shoelaces 1 and Long Split Telescope layouts are assessed as low risk in this category for these reasons.

4.7 Stray light performance

The corner optical layout determines certain scattering angles of interest between different regions of the corner interferometer. In particular, a low AOI on the BS may increase the level of forward-scattered light from one arm of the short Michelson to the other, as well as directly into the counter-propagating direction. Furthermore there are important considerations relating to ghost beams, especially at the ITM, that are indirectly dependent on the corner layout. At this stage stray light considerations are not given high priority in the down selection process, but where distinctions can be made between different layouts in this regard we aim to record those here. The stray light team is currently pursuing some of the questions raised here.

Almost all of the layouts presented here could benefit from the inclusion of a lens figured into the ITM AR surface. This allows the beam to start converging sooner upon exiting the arm cavities, which makes it easier to keep the SEC short. However, this feature is more critical for the Crab layouts than others. This is because they otherwise require a strongly converging mirror under a $\sim 22^{\circ}$ AOI, which must be toroidal in nature to avoid introducing a large astigmatism. One of the concerns about a strong ITM lens (with AR surface radius of curture around 40 m) is that AR surface reflections (a.k.a. ghost beams) from within the PRC will diverge rapidly, causing stray light concerns. Preliminary studies have shown that with quite large wedge angles on the ITM, these ghost beams can be separated by several beam radii from the main beam by the time they encounter the next mirror. However, this remains a topic of study, and for the time being we give these layouts a mid-low risk rating for this category.

Another stray light consideration is the AOI at the BS. The lower BS AOI layouts may suffer from increased forward scatter through the BS from one arm of the short Michelson to the other, and from the PRC directly to the SEC, when compared to the traditional 45° BS AOI layouts. It also may increase the level of scatter from the short Michelson arms back into themselves via the BS, and from PRC/SEC back to themselves via the BS. This is also a topic of contemporary study, so for the time being we give all low BS AOI layouts a mid-low risk rating for this category.

4.8 Infrastructure impacts

This consideration is difficult to quantify at this stage, but all different layouts will have to be compatible with a realistic and affordable vacuum infrastructure. In particular, low BS AOI layouts present new challenges for vacuum system design. Where possible, we identify impacts on the vacuum infrastructure, and any knock-on impacts on the corner building.

In terms of risk rating, we take the conservative approach of assigning all 45° layouts as low risk. All existing GW detectors have been able to configure the vacuum infrastructure to accommodate interferometers with layouts like these. The aLIGO infrastructure in particular has proven very flexible for allowing upgrades, which is a great advantage we also seek to maintain for CE as we envisage future upgrades beyond the initial CE interferometers. We assign a mid-low risk in this category for the low BS AOI layouts, primarily because of the lack of experience with designing vacuum infrastructure around them. It is worth noting though that some preliminary designs based around the Long Crab 1 layout have shown some potential advantages. It is conceivable that some of the smaller core optics could share vacuum chambers and even ISI tables (e.g. PRM and PR3, PR2 and SEM, MY1 and MX2,

MX1 and MY2). Also, it may be convenient to access several diagnostic beams at the same location as the interferometer output [8].

5 Additional considerations for optical layouts

There are some considerations which are either unique to specific optical layouts, or are effectively equal for all layouts but still worth noting at this stage. Such considerations are therefore are not appropriate to include as part of a direct comparison between layouts, but are discussed separately in this section.

5.1 Higher-order spatial mode coupling

With an arm cavity free spectral range of just 3.75 km, effectively all higher-order spatial mode resonances will lie in the detection band. The effect of coupling to higher-order modes will therefore partly be to dephase the squeezed vacuum, and therefore inject 'anti-squeezing' at frequencies around the higher-order mode resonances, as shown in Ref. [9]. This phenomenon places a strong emphasis on optimizing wavefront matching between the SEC and the arm cavities. This is a contemporary topic of study, and at the current time the impact of SEC geometry and some other design details is not fully understood. However, we expect that the most critical factors for mitigating the problem are largely layout independent, with the exception of the considerations already made for SEC loss. It is therefore beyond the scope of this note to compare individual layouts with regard to this consideration.

5.2 Aberrations

Simple ABCD matrix calculations for Gaussian beam propagation rely on the approximation that spherical surfaces are indistinguishable from parabaloid surfaces. In this approximation, spherically curved mirrors or lenses are perfect imaging optics for Gaussian beams with parabolic wavefronts, and therefore cause no mode scattering, or aberration-induced optical losses. However, with strict SEC loss targets, and high susceptibility to higher-order mode scattering, these approximations come under renewed scrutiny for the CE optical design. Generally speaking, extending to the next order in the approximation includes the effect of the Seidel aberrations, most notably spherical aberration. Preliminary studies based on early SEC designs indicate that the spherical aberration should not be a limiting factor for SEC loss [10], but this consideration should be borne in mind as the designs progress after down selection.

5.3 ITM lens

Many layouts would benefit from the addition of an ITM lens, achieved by figuring the AR surface of the ITMs. It allows the beam to converge towards the BS immediately upon exiting the arm cavities, reducing the "dead space" over which no convergence occurs, but which still contributes to the SEC length. For the Crab 1 layouts, an ITM lens would potentially allow MX/Y2 to be flat optics, which would go a long way to mitigating the astigmatism concerns without requiring toroidal mirrors.

Including ITM lenses is however a significant design departure from the aLIGO interferometers, and therefore requires careful study [†]. Some of the technical impacts of opting for a strong ITM lens are addressed in Ref. [11]. A draft design for an ITM with 40 m AR surface radius of curvature has also been produced [?]. These preliminary studies have not identified any fundamental roadblocks to producing such ITMs, but it remains an active topic of study at this time. It is worth noting that a strong ITM lens with a wedge angle produces astigmatism. If the wedge is oriented vertically, however, the astigmatism produced is of the opposite sign to that produced by curved mirrors with a horizontal plane of incidence and so these could be designed to cancel out [12]. A wedge also provides a means for lateral motion of the ITM to couple into the auxiliary length degrees of freedom. This should be considered when calculating requirements for the ITM seismic isolation system.

5.4 Toroidal mirrors

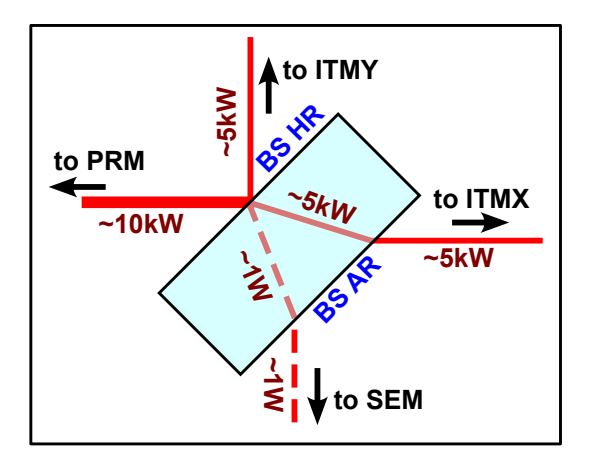
The alternative for avoiding the impact of the $\sim 14\%$ different effective radius of curvature of mirrors under $\sim 22^\circ$ AOI in the low BS AOI layouts is to use *toroidal* mirrors. For example in the Long Crab 1 layout, if MX2 and MY2 are to have any significant focusing power, they must be made to have similar *effective* radii of curvature in tangential and sagittal axes. This means that the tangential plane radius of curvature have to differ by 14% when viewed at normal incidence. Initial discussions have indicated that such mirrors can in principle be produced, although we have not yet performed a deatiled analysi of their likely cost and performance.

Although some layouts could rely heavily on toroidal mirrors, it should also be mentioned that the level of astigmatism in the aLIGO recycling/extraction cavities (which are designed with relatively low AOI on all curved mirrors) could already pose a problem for the CE requirements on SEC loss. The impact on the quantum noise limited sensitivity around higher-order mode resonances in the arm cavity could be even more severe. It may be beneficial therefore to investigate astigmatism-free designs, possibly including the use of toroidal mirrors in multiple locations throughout the corner interferometer, regardless of layout. Some preliminary studies on astigmatism-free designs are reported in Ref [12].

5.5 Beamsplitter orientation

In the context of discussions around BS thermal lensing, we have considered the alternative orientation for the BS HR and AR surfaces, with respect to that used in aLIGO. The two possible orientations, 'regular' and 'flipped' are shown in Fig. 3, with BS port labels which are appropriate for the aLIGO layout. The proposed advantage of the flipped layout was that the SEC paths would encounter fewer AR coating passes, and therefore lower optical losses, in this configuration [13, 14]. The regular orientation has 1 BS AR surface encounter for the beam traversing between SEM and ITMY, and 2 for the beam traversing between SEM and ITMX, for a total of 3 encounters. In the flipped configuration, the beam traversing between SEM and ITMY still encounters the AR surface once, but the beam traversing between SEM and ITMX does not encounter the AR surface at all, for a total of just 1 encounter.

[†]It is notable that AdVirgo is designed with lenses in the compensation plates, however.



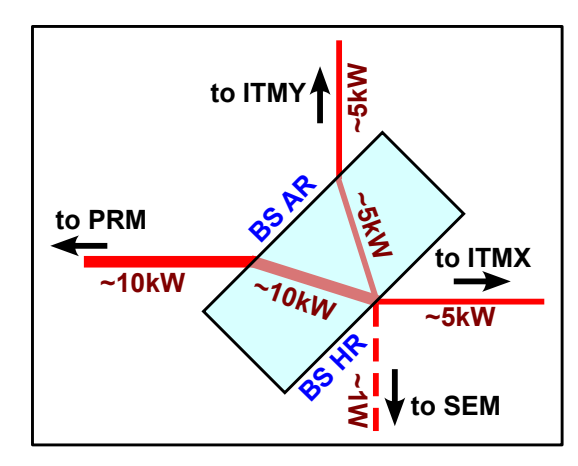


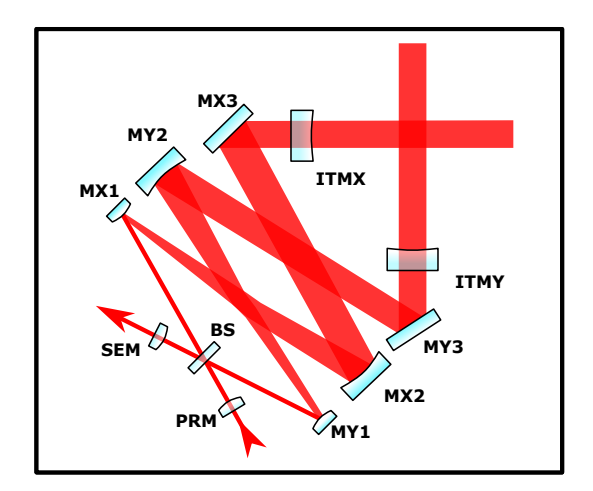
Figure 3: Illustration of the two possible orientations of the BS within the corner interferometer in the context of the aLIGO layout. The 'regular' orientation, used in aLIGO itself, is shown on the left with an estimated total power traversing the BS substrate of 5kW in each direction in CE. The 'flipped' orientation is shown on the right, with 15kW traversing the BS substrate in each direction.

Another consideration is the thermal lensing due to optical power absorption in the BS. As shown in Fig. 3, the optical powers in the two individual substrate paths differ by 5 kW in either orientation, but in the flipped orientation the total substrate absorbed power is three times as high as in the regular orientation. The optical power involved in AR surface encounters is also three times as high for the flipped configuration, exacerbating the effects of AR coating absorption and resulting thermal lensing in this configuration.

Although detailed thermal modeling has not been performed for the flipped orientation, a general preference for lower total power absorption at the BS, and an estimate that AR coating optical losses will not be a limiting factor, is enough for the present time to encourage us to stick with the regular orientation.

5.6 Arm cavity beam crossing point

Not heretofore discussed is the decision of whether the arm cavity beams cross before or after transmission out of the cavities through the ITMs. In all current GW detectors, the beams cross after transmission out of the cavity. In all of the low AOI layouts illustrated in Fig 1, the arm cavity beams are shown to cross before exiting the cavity. This potentially allows a shorter distance before the next folding mirror is encountered, thus helping to maintain a short SEC, once again by reducing the "dead space" over which no beam convergence occurs. However, in the case that ITM lenses are used to begin the beam convergence, the motivation to have beams cross within the arm cavities will be reduced. There may also be stray light implications to having the beams cross at high power within the arm cavities, but these have not yet been explored. We note that it is also possible to configure the 45° AOI layouts to have the beams cross within the arm cavities, although the potential benefits to doing so are not obvious. Likewise it is also possible to configure the low BS AOI layouts to have the beams cross outside the arm cavities. This decision in the end may come down



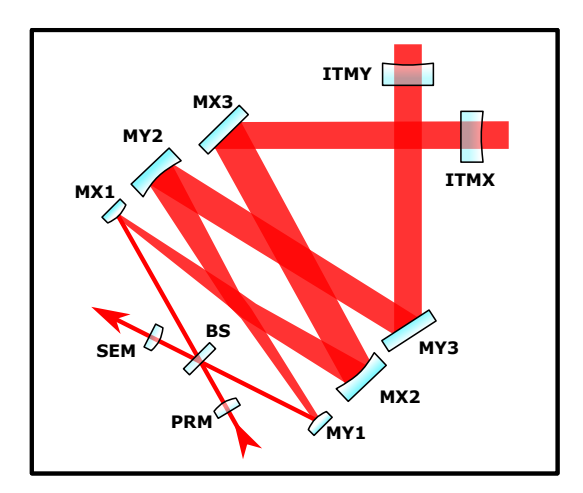


Figure 4: Illustration of the two arm cavity beam crossing options for the Shoelaces 1 layout. On the left, the beams cross before exiting the arm cavities through the ITMs. On the right, the beams cross after exiting the arm cavities through the ITMs.

to detailed analysis of the optimal locations for the large folding mirrors (e.g. MX/Y2 for Long Crab 1) relative to the ITMs.

6 Preferred layouts and design concepts

The evaluation of risks associated with the different layouts led to the identification of two most promising candidates for further study: Long Reverse aLIGO and Long Crab 1. Each of these layouts, but especially Long Crab 1, carries some specific design requirements and additional design choices with them. In this section we give a brief overview of how each of the preferred layouts might look as we proceed toward the more detailed preliminary optical design. This section does not constitute even a preliminary design for either layout, but merely hints at some of the more major features of each. Detailed preliminary design documentation will be completed in due course for each of the preferred layouts.

6.1 Long Crab 1

The Long Crab 1 layout offers the primary benefits of low AOI at the BS, and full MSC actuation authority for the PRC and SEC, as well as the common and differential arm modes. The biggest concern for this layout is the issue of astigmatism due to either the $\sim 22^{\circ}$ AOI on MX/Y2, or the use of a strong ITM lens with a wedge. At this stage we conclude that the strong ITM lens is a more realistic design feature than strongly toroidal MX/Y2 mirrors. In this case, we allow MX/Y2 to be flat, such that the $\sim 22^{\circ}$ AOI has no impact on astigmatism of the beams. In this sense, the Long Crab 1 design becomes something of a hybrid between Long Crab 1, Long Shoelaces 1, and ITM Lens layouts. We keep the name Long Crab 1 though, because it remains topologically most similar to that layout.

We also find it likely that a design with the beams crossing within the arm cavity is preferred from the SEC length point of view. If serious difficulties are encountered with this choice, we may revisit and consider more traditional beam crossing outside the arm cavities. Especially

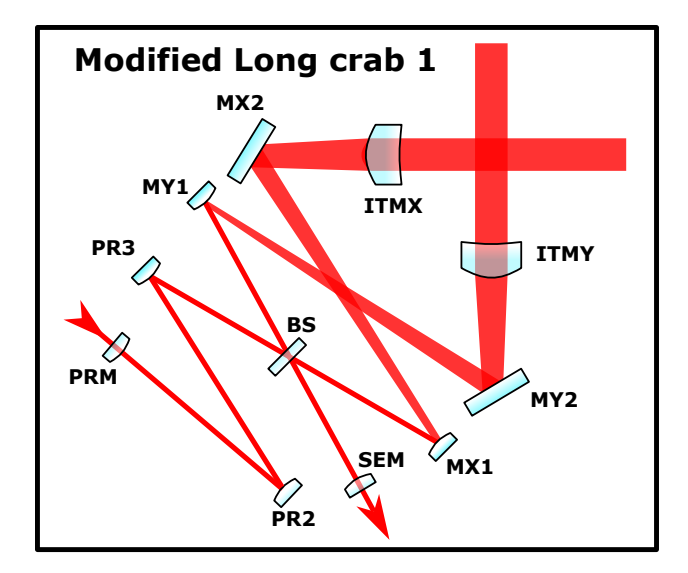


Figure 5: A cartoon sketch of the Long Crab 1 layout, modified to include the strong ITM lens and flat MX/Y2 mirror design features.

with the strong ITM lens, the region immediately outside of the arm cavity is no longer "dead space" from the beam convergence point view, which relaxes the drive towards an intra-cavity beam crossing design.

Given these additional considerations, Fig. 5 shows a cartoon sketch of how this modified Long Crab layout is more likely to look, compared with the equivalent sketch in Fig. 1. At the time of writing, Ref. [8] represents the most advanced reference for the Long Crab 1 design. More detailed design documentation will follow in due course, and should be linked via the CE DCC to this and other documentation.

6.2 Long Reverse aLIGO

The Long Reverse aLIGO offers the primary benefits of compatibility with a more traditional vacuum envelope, full MSC actuation authority for the PRC and SEC, as well as the common and differential arm modes, and reduced reliance on toroidal mirrors or ITM lens. The ITM lens may still offer SEC length reduction benefits, but it is not seen as being so critical for this layout as for the Long Crab 1 layout. There are no significant additional considerations for this layout, so the cartoon sketch shown in Fig. 1 remains appropriate at this stage.

It is worth mentioning that while at first glance this layout seems quite similar to the aLIGO layout, the location of the telescopes within the short Michelson arms instead of within the PRC and SEC makes a significant difference. The novelty brings with it some potential risk, but it does allow for a much more manageable beam size at the BS, and it gives a suitable array of MSC actuation sites. It is also possible that the vacuum infrastructure designed around this layout may also be compatible with an aLIGO-like layout as a deep backup option, should insurmountable difficulties be encountered further down the line with the Long Reverse aLIGO layout.

Parameter	Value	Units
Arm cavity length	40	km
Arm cavity finesse	450	
Arm cavity waist radius	69	mm
ITM beam radius	120	mm
ITM HR R_c †	-29.87	km
In-arm arm cavity q parameter [‡]	20 + i 14	km
In-corner arm cavity q parameter§	16.7 + i8.1	km

Table 1: The CE 40 km arm cavity parameters assumed for this study.

A Optical design boundary conditions and assumptions

Some of the preceding discussion relies on assumption about the parts of the CE design which are layout independent, i.e. primarily the arm cavities. The assumed arm cavity parameters, along with other parameters and boundary conditions for the corner layout are summarized in Ref. [15]. We reproduce the most relevant arm cavity parameters to the discussions in Tab. 1 here for convenience.

B Calculation of the arm cavity mode in the corner interferometer

The arm cavity mode assumed in App. A has a Rayleigh range of $z_{R_{ARM}} = \frac{\pi w_{0_{ARM}}^2}{\lambda} = 14.06 \,\mathrm{km}$. When propagating this mode into the corner interferometer, we should in general not ignore then influence of the ITMs HR surface curvature. The combined HR, substrate and AR surface ABCD matrix for the ITM is given by

$$M_{\text{ITM}} = M_{\text{ITMAR}} M_{\text{ITMSub}} M_{\text{ITMHR}} = \begin{bmatrix} 1 & 0 \\ \frac{n_{\text{glass}} - 1}{R_c^{\text{HR}}} & 1 \end{bmatrix} \begin{bmatrix} 1 & t_{\text{ITM}}/n_{\text{glass}} \\ 0 & 1 \end{bmatrix} \begin{bmatrix} 1 & 0 \\ \frac{1 - n_{\text{glass}}}{R_c^{\text{AR}}} & 1 \end{bmatrix}, \quad (5)$$

where for now we assume normal incidence at both surfaces. In the ITM case, the propagation through the substrate thickness $t_{\rm ITM}$ has negligible effect on the beam parameter, so we can simplify the ABCD matrix to

$$M_{\text{ITM}} = \begin{bmatrix} 1 & 0 \\ \frac{n_{\text{glass}} - 1}{R_c^{\text{HR}}} & 1 \end{bmatrix} \begin{bmatrix} 1 & 0 \\ \frac{1 - n_{\text{glass}}}{R_c^{\text{AR}}} & 1 \end{bmatrix} = \begin{bmatrix} 1 & 0 \\ \frac{1 - n_{\text{glass}}}{R_c^{\text{AR}}} + \frac{n_{\text{glass}} - 1}{R_c^{\text{HR}}} & 1 \end{bmatrix}.$$
 (6)

For the special case of a flat AR surface, this reduces to simply the ABCD matrix of the HR surface. Using $n_{\rm glass}{=}1.45$ and with $R_c^{\rm HR}=-29.87\,{\rm km}$, we arrive at

$$M_{\rm ITM} = \begin{bmatrix} 1 & 0 \\ -1.5 \times 10^{-5} \,\mathrm{m}^{-1} & 1 \end{bmatrix}. \tag{7}$$

[†]Using the convention that a negative value signifies a concave surface viewed by the beam arriving from the ETM.

[‡]Evaluated at the HR surface of the ITM, assuming a flat AR surface.

[§]Evaluated at the AR surface of the ITM, assuming a flat AR surface.

The arm cavity q parameter is then modified from $q_{\rm ARM}=(20+i14.06)\,{\rm km}$ to $q_{\rm ARM}^{\rm corner}=(16.7+i8.1)\,{\rm km}$. However, the calculation in Sec. 4 for the ITM Lens layout makes the thin lens assumption for the entire ITM. In the case of any reasonable ITM lens design for this layout, the focal power of the AR surface will vastly outweigh the (negative) focal power of the HR surface. Thus, for calculating the overall ITM lens focal length needed for a given Rayleigh range, and the resulting SEC length, it is suitable to use the unmodified $q_{\rm ARM}=(20+i14.06)\,{\rm km}$ value. On the other hand, a calculation of the appropriate ITM AR surface curvature $R_c^{\rm AR}$ must account independently for the refractive power of the HR surface.

References

- [1] Huy-Tuong Cao. Thermal lensing compensation of beamsplitter under different angles of incidence. Technical report, Cosmic Explorer DCC. Available at TBD.
- [2] Kevin Kuns. Impact of signal extraction cavity length on postmerger sensitivity for Cosmic Explorer. Technical report, Cosmic Explorer DCC. Available at TBD.
- [3] Kevin Kuns. Impact of signal extraction cavity optical losses on Cosmic Explorer sensitivity. Technical report, Cosmic Explorer DCC. Available at TBD.
- [4] Satoshi Tanioka, Bin Wu, Stefan Ballmer, and Kevin Kuns. Thermorefractive noise limitation on Cosmic Explorer's beamsplitter size. Technical report, Cosmic Explorer DCC. Available at https://dcc.cosmicexplorer.org/CE-T2400004.
- [5] Kevin Kuns. Bulk acoustic mode frequencies of the beamsplitter. Technical report, Cosmic Explorer DCC. Available at https://dcc.cosmicexplorer.org/CE-T2300012.
- [6] Matthew Todd and Stefan W. Ballmer. Beamsplitter in a strongly convergent telescope. Technical report, Cosmic Explorer DCC. Available at https://dcc.cosmicexplorer.org/CE-T2300014.
- [7] Aidan Brooks, Rana Adhikari, Stefan Ballmer, Lisa Barsotti, Paul Fulda, Antonio Perreca, and David Ottaway. Active wavefront control in and beyond Advanced LIGO. Technical report, LIGO DCC. Available at https://dcc.ligo.org/LIGO-T1500188.
- [8] Matthew Todd and Stefan Ballmer. Draft: Initial conceptual layout Cosmic Explorer corner station. Technical report, Cosmic Explorer DCC. Available at https://dcc.cosmicexplorer.org/CE-G2400048.
- [9] Kevin Kuns. Impact of higher-order mode arm cavity resonances in Cosmic Explorer. Technical report, Cosmic Explorer DCC. Available at TBD.
- [10] Liu Tao, Sagar Gupta, and Paul Fulda. Higher-order mode scattering power loss due to spherical aberration. Technical report, Cosmic Explorer DCC. Available at https://dcc.cosmicexplorer.org/CE-T2400011.
- [11] Sagar Gupta, GariLynn Billingsley, Jonathan Richardson, and Stefan Ballmer. Considerations for a strong ITM lens in the Cosmic Explorer optical design. Technical report, Cosmic Explorer DCC. Available at TBD.

CE-T2400012-01

- [12] Sagar Gupta and Paul Fulda. Astigmatism considerations for CE recycling/extraction cavity design. Technical report, Cosmic Explorer DCC. Available at TBD.
- [13] Hiro Yamamoto. Effects of different sizes of BS for A+. Technical report, LIGO DCC. Available at https://dcc.ligo.org/LIGO-G1800155.
- [14] Hiro Yamamoto. Beam splitter in aLIGO. Technical report, LIGO DCC. Available at https://dcc.ligo.org/LIGO-G1500634/public.
- [15] Paul Fulda, Kevin Kuns, and Alena Ananyeva. Cosmic Explorer corner layout boundary conditions. Technical report, Cosmic Explorer DCC. Available at https://dcc.cosmicexplorer.org/E2300006.